Effect of creep on the Young's modulus of aramid fibres

A. K. Rogozinsky and S. L. Bazhenov*
Institute of Chemical Physics, Kosygin St. 4, 117977 Moscow, USSR
(Received 26 March 1991; accepted 16 April 1991)

The effect of creep and recovery on the Young's modulus of different aramid fibres was investigated by an acoustic method. Creep leads to the growth of the Young's modulus of up to 215 GPa. Some of the difference between moduli values obtained by the acoustic and mechanical methods can be traced to fibre viscoelastic deformation. The dependence of the reciprocal Young's modulus on the creep strain is described by a straight line, the slope of which is practically independent of stress and temperature. Creep and recovery may be described as a thermoactivated transition between two energy states that have different elasticities of the polymer chain. These states are supposed to be the straightened molecule and a molecular kink.

(Keywords: aramid fibres; creep; recovery; Young's modulus; acoustic method)

INTRODUCTION

The Young's modulus is usually considered a constant parameter characteristic of the material. In elastic–plastic metals and isotropic polymers the inelastic component of deformation leads to some reduction of the stress–strain curve slope, i.e. to a decrease of the modulus compared to its initial value. On the contrary, in oriented polymer fibres Bessonov and Rudakov[1] have observed some increase in elasticity during loading. This effect was observed in aramid poly(amidobenzimidazole) (PABI)[2–6], poly(phenylene terephthalamide) (PPTA)[4,6,7] and Du Pont Kevlar 49 (PPTA) fibres[8–11] during loading[2,3] and creep[4,5]. The methods used were mechanical testing[10], an acoustic method[2,4–6,11], X-ray diffraction[3,8,9] and spectroscopic analysis[12,13]. The increase in modulus found during loading was explained by the progressive improvement of crystalline orientation[2,3,8] and by the orientation of supramolecular 'pleated sheet' structure[10].

Apart from direct measurement of the Young's modulus by mechanical testing, the Young's modulus may be determined by measurement of acoustic wave velocity, $E_d = \rho c^2$, where ρ is the material density and c is the velocity of the acoustic wave. Measured by this method, the 'dynamic' modulus is sometimes higher than the 'tangent' $E_t = \Delta\sigma/\Delta\varepsilon$. In light of these two facts, the main objectives of the present work were to study the effect of the viscoelastic part of the deformation on the Young's modulus and to find the cause of the difference in modulus values measured by the acoustic and mechanical methods.

EXPERIMENTAL

The subjects of this investigation were 530 denier PABI yarns (trademark SVM[14]), 530 denier PPTA yarns (trademark Terlon[14]), 930 denier Armos[14] and 200 denier Kevlar 49 (PPTA) yarns.

The ends of the samples (single fibre or a yarn) were fixed in special conical-shaped moulds, which were filled with liquid epoxy resin EDT-10. After curing of the resin, the ends of the samples formed conic heads, which were used to load the fibres and to induce acoustic waves. The working length of the samples was 1 m. The specimens were loaded by the addition of weights. The acoustic wave velocity was determined by measuring the time taken by the leading edge of the acoustic pulse to reach the input strain-gauge transducer. The frequency of the acoustic wave was 50 kHz (in the range 3–200 kHz the dynamic Young's modulus E_d does not depend on the wave frequency[5]). The pulse repetition frequency was 100 Hz. Taking into account the fibre elongation under stress, the acoustic wave velocity was calculated from the equation $c = (L_0 + \Delta L)/T$, where $L_0 = 1$ m, ΔL is fibre elongation and T is time taken by the pulse to pass through the sample. The decrease of the fibre density during its straining due to the Poisson effect was not taken into account.

Water was removed from the fibres by specially dehumidified air at 110°C. The samples were preliminarily loaded before testing. After unloading, some straining that could not be annealed even after heating at 150°C for 40 h has remained (*Figure 1*).

The value of the preliminary stress was limited according to the probability of fibre breakage. As a rule the prestress value was equal to 1500 MPa for PPTA and Kevlar 49, and to 2200 MPa for PABI and Armos yarns. In the case of PABI and Armos fibres some measurements have been taken at 2500 MPa stress. The temperature usually did not exceed 110°C.

RESULTS

All the aramid fibres under observation (PABI, PPTA, Armos and Kevlar 49) revealed creep. To study the effect

* To whom correspondence should be addressed at: Department of Marcomolecular Science, Case Western Reserve University, Cleveland, Ohio 44106, USA

0032-3861/92/071391-08

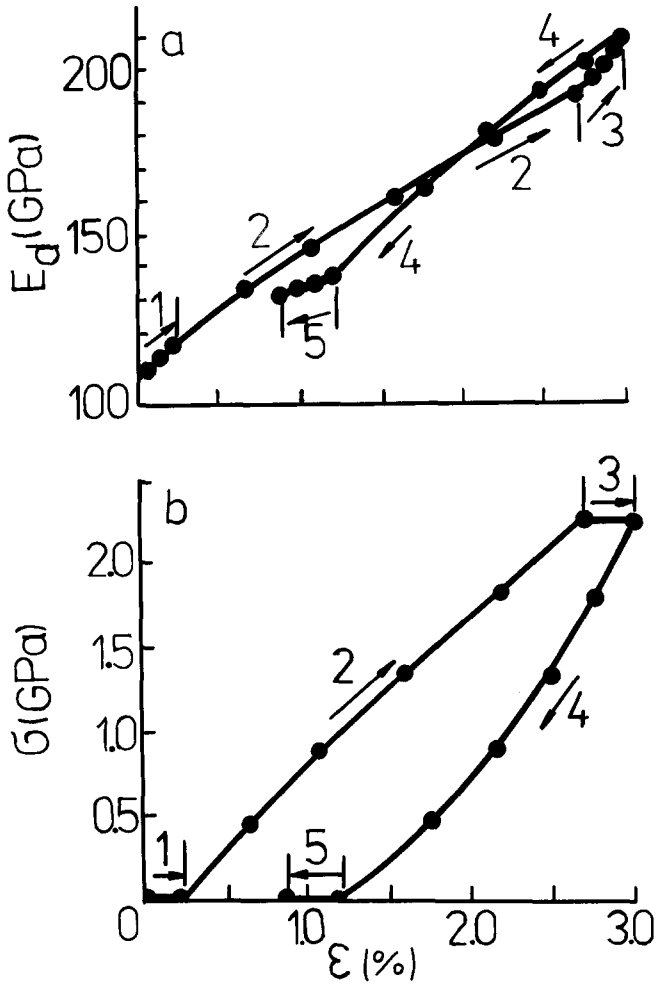

Figure 1 Dynamic modulus E_d (a) and stress σ (b) of PABI yarn plotted against strain during preliminary loading: (1) drying; (2) loading; (3) creep under stress; (4) unloading; (5) recovery and annealing

of creep on the Young's modulus, it was necessary to test fibres that have sufficiently high elongation during creep. As the creep rate is highest in PABI fibres, the experiments were mainly carried out using these fibres.

Figure 1 shows the loading (2) and creep (3) lead to significant growth of the PABI fibres' Young's modulus, which reached 215 GPa. This value is very close to the theoretical limit 210–250 GPa[15,16]. The effect of unloading (4), recovery and annealing (5) is opposite. Fibre elongation (~0.3%) and increase of modulus (~8 GPa) during drying (1) also could be noted.

In the first loading cycle the elongation is the sum of three parts: (1) elastic; (2) viscoelastic, which could be annealed; (3) inelastic, which could not be annealed (at 150°C). According to *Figure 1* after annealing the final modulus is higher than the initial one before loading. Consequently, irreversible strain leads to some modulus growth. In subsequent loading cycles the creep elongation could be completely annealed if the stress and temperature were not higher than at prestress. The modulus in this case is also reversible. Thus prestressing permits to avoid irreversible strain during subsequent loadings.

Figure 2 shows that the effect of creep on the Young's modulus of a single PABI fibre and a yarn consisting of 300 fibres is similar. However, there is some difference between the fibre and the yarn. The cause of this difference may be inaccuracy in the determination of the fibre diameter. Since testing of a single fibre is associated with some extra experimental difficulties (measurement of very low weights, friction in loading device, danger of fibre breakage owing to careless treatment, and the necessity of precise diameter measurement), yarns were mainly tested.

To obtain a significant fibre strain at not very high stress, much time is needed. To shorten the measurement time, a special loading technique as shown in *Figure 3* was used. After observing creep at 2250 MPa stress, the weights were gradually removed. On varying the time of initial loading (at 2250 MPa), different fibre lengths during unloading at each load were obtained. As a result, the correlation between viscoelastic strain increment and the Young's modulus were studied at several stresses.

Figure 4 shows that dynamic modulus E_d plotted against increment in viscoelastic strain does not depend on the way the sample was loaded. The results are ascribed by the same curve for creep, for recovery and for loading according to *Figure 3*. Hence, at fixed stress, fibre strain unambiguously determines its modulus and vice versa. As a consequence, the dependence of strain on stress and modulus, $\varepsilon(\sigma, E)$, does not depend on the fibre history and the loading method. For this reason, below the loading method will not be noted. At high stresses (>1500 MPa) the results are mainly obtained for creep; at low stresses (<500 MPa) for recovery; and at intermediate stresses for loading according to *Figure 3*.

DYNAMIC AND TANGENT MODULI CORRELATION

Figure 5 shows modulus E plotted against the fibre strain, ε for three different loading methods. The loading

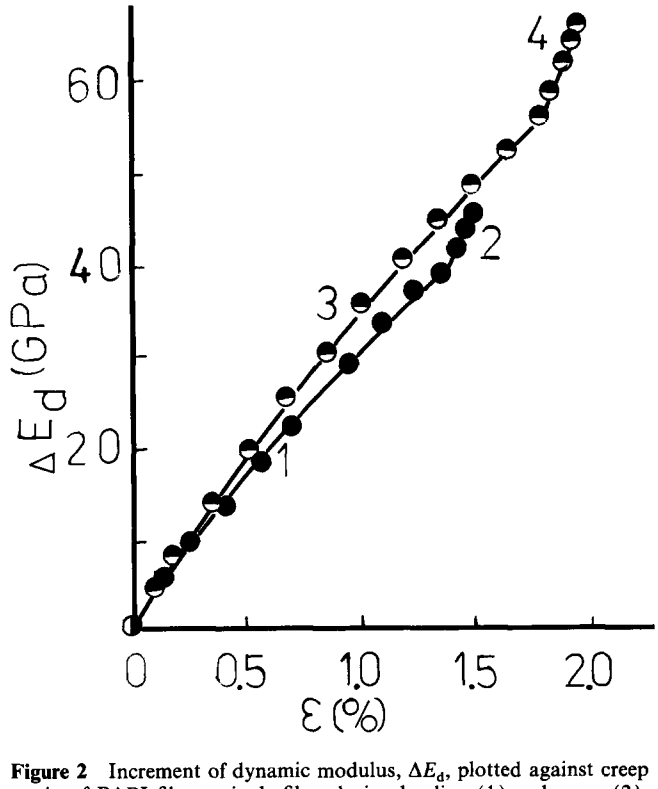

Figure 2 Increment of dynamic modulus, ΔE_d, plotted against creep strain of PABI fibres: single fibre during loading (1) and creep (2); yarn consisting of 300 parallel fibres during loading (3) and creep (4)

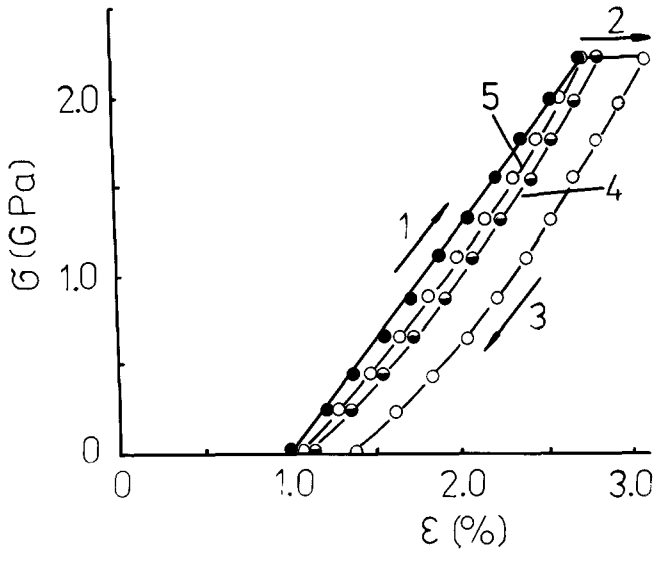

Figure 3 PABI yarn stress σ *versus* strain ε: loading (1); creep (2); unloading after different periods of creep (3, 4) and immediately after loading (5). Arrows show the directions of loading, creep and recovery

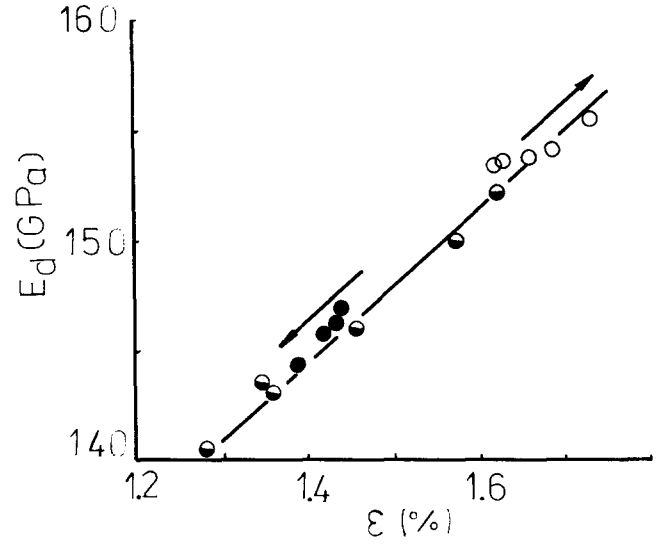

Figure 4 PABI yarn dynamic modulus E_d plotted against strain ε: (○) creep; (●) recovery; (◒) loading according to *Figure 3*; $\varepsilon = 0.45$ GPa, $T = 22°C$

methods were chosen so as to provide different creep rates at the moment when a subsequent weight is added.

In the first case, subsequent weights were added after every 10–15 s (which are needed for measurements of acoustic wave velocity). This method models the loading with constant elongation velocity. Values of tangent and dynamic moduli do not coincide and the difference increases with stress (curves 1 and 2). The dynamic modulus E_d in this case monotonically increases with strain (curve 1) while E_t has a maximum (curve 2).

In the second loading method the weights were added after 10 min. The creep rate in this case is very low at the moment when a subsequent weight is added. Hence, viscoelastic elongation, after addition of the next weight, was much lower than in the first case. The dependence of the dynamic modulus practically coincides with that of the first loading method (curves 1 and 3). On the contrary, the dependence of the tangent modulus (curve 4) is essentially different from that in the first technique. The difference between the dynamic and tangent moduli values in this loading method is much lower (curves 3 and 4) than in the first case. Some of the difference between E_t and E_d values may be explained by creep recommencing after addition of subsequent weights.

In the third case, the modulus was measured during unloading. The weights were removed at a constant rate (every 10–15 s). In this case the creep rate (especially at high stresses) was even lower than that with the second loading technique. At lower stresses recovery appeared. The dynamic modulus (curve 5) again coincides with that in the first two loading techniques. Thus the dynamic modulus practically does not depend on the loading method. At high stresses, when the creep rate during unloading could be neglected, the tangent modulus is found to be very close to the dynamic modulus (two points on curve 6). At lower stresses, recovery of the fibre length leads to a significant decrease of E_t (curve 6). The behaviour of the tangent modulus confirms the supposition that the difference between E_t and E_d is due to the effect of creep on E_t.

Thus increase in creep rate does not influence the dynamic modulus and leads to a decrease in the tangent modulus. The cause is evident. As the frequency of the acoustic wave is very high (50 kHz) the creep elongation for times $\sim 10^{-5}$ s could be neglected, and E_d is determined completely by the polymer elasticity. On the contrary, values of the tangent modulus essentially change with the variation in the creep rate. To explain this effect, we note that the tangent modulus is determined by total fibre elongation under stress, $E_t = \Delta\sigma/(\Delta\varepsilon_e + \Delta\varepsilon^*)$, where $\Delta\varepsilon_e$ and $\Delta\varepsilon^*$ are the increments of elastic and viscoelastic strain. If the creep rate is low and $\Delta\varepsilon^*$ can be neglected, then $E_t \simeq E_d$. But if during creep or recovery $\Delta\varepsilon^*$ cannot be neglected, $E_d > E_t$. Thus, the difference between E_d and E_t is due to the creep. The higher the creep rate, the greater the difference.

MODULUS–DEFORMATION CORRELATION

The dependence of the dynamic modulus on strain increment during creep is not linear. *Figure 6* shows that

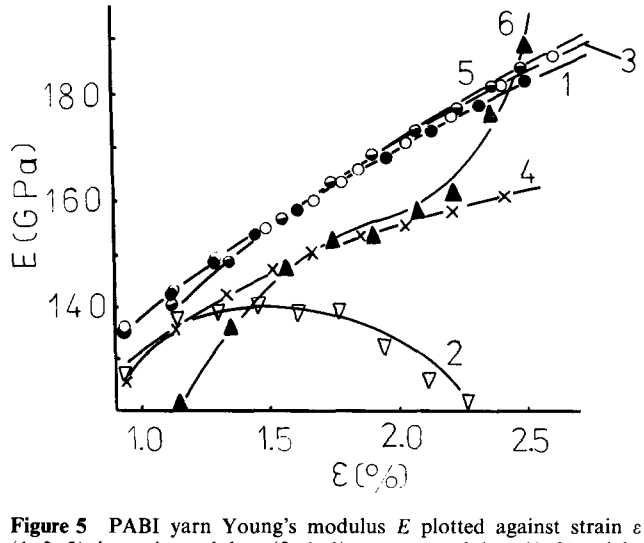

Figure 5 PABI yarn Young's modulus E plotted against strain ε: (1, 3, 5) dynamic modulus; (2, 4, 6) tangent modulus; (1, 2) weights are added after every 10–15 s; (3, 4) weights are added after 10 min; (5, 6) unloading

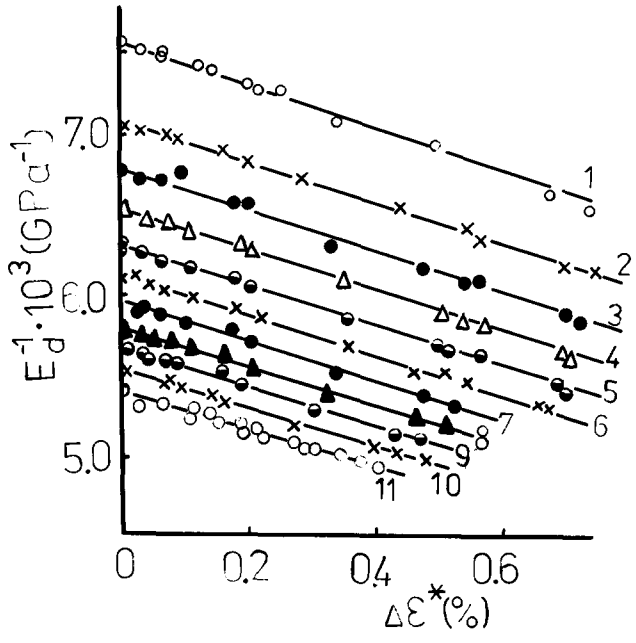

Figure 6 Reciprocal dynamic modulus $1/E_d$ of PABI yarn plotted against creep strain increment $\Delta\varepsilon^*$: (1, 2) recovery; (3–9) loading according to *Figure 3*; (10, 11) creep. Stress is equal 0 MPa (curve 1), 224 (2), 448 (3), 672 (4), 896 (5), 1120 (6), 1344 (7), 1568 (8), 1792 (9), 2016 (10) and 2240 MPa (11)

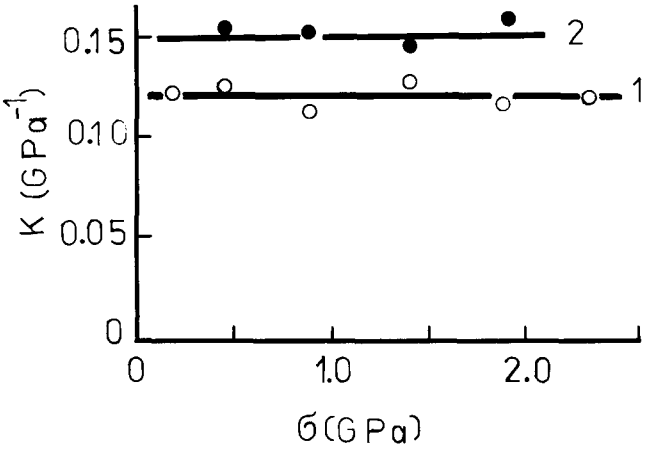

Figure 7 Coefficient K in equation (1) plotted against stress ε for PABI yarn at 22°C (1) and 110°C (2)

this dependence does become linear in the following coordinates: reciprocal modulus $(1/E_d)$ *versus* creep strain increment $(\Delta\varepsilon^*)$[6]. Thus:

$$1/E_d = 1/E_0 - K\,\Delta\varepsilon^* \qquad (1)$$

where K is the slope of the straight line and E_0 is the initial modulus.

Figure 7 shows that the slopes of straight lines K in *Figure 6* do not depend on the creep stress. *Figure 8* shows that K increases slightly with temperature.

Figure 9 shows $1/E_d$ plotted against the total strain ε (elastic plus viscoelastic) for different creep stresses. The experimental data are the same as in *Figure 6*. This dependence is described by several parallel straight lines corresponding to different stresses. These lines in a wide range of stresses (225–1350 MPa) converge to a single straight line:

$$1/E_d = 1/E_0 - K\varepsilon \qquad (2)$$

where $E_0 = 115$ GPa, K is constant (0.12 GPa^{-1}) and ε is the total strain.

The increase of Young's modulus under load is typical for all aramid fibres. In Kevlar 49, PPTA and Armos fibres, moduli values equal to 195, 190 and 205 GPa respectively have been registered.

Figures 10 and *11* demonstrate that the dependence of reciprocal modulus on the creep strain is linear not only for PABI but also for PPTA, Armos and Kevlar 49 fibres. The test temperature was elevated with the aim of obtaining high enough fibre elongation during creep. For PPTA and Kevlar 49 fibres, the K values (0.30 and 0.32) are very close. This may be explained by similar chemical structure of the fibres. The K value of Armos fibres (0.35) is close to that for PPTA and Kevlar 49.

MODEL

We failed to explain the linear $1/E_d$ *versus* $\Delta\varepsilon^*$ correlation by the Takayanagi model[17] in accordance with which a polymer is a sequence of amorphous and crystalline regions with different Young's moduli, where the modulus of the amorphous regions is proportional to the part of loaded ('passing') molecules[18,19]. This correlation may be explained only if it is supposed that: (1) the polymer molecule is a chain of equivalent fragments, which are

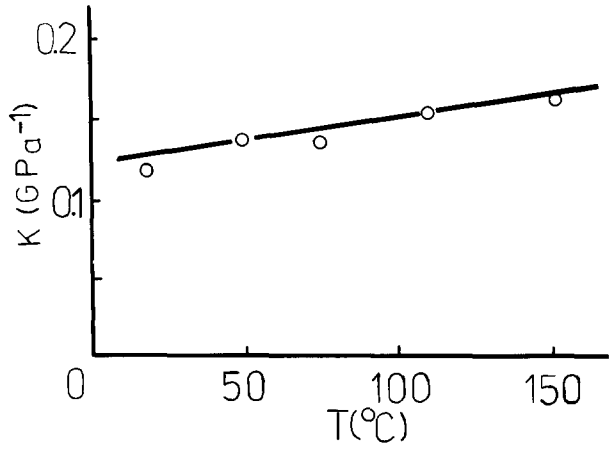

Figure 8 Coefficient K plotted against creep temperature T for PABI yarn

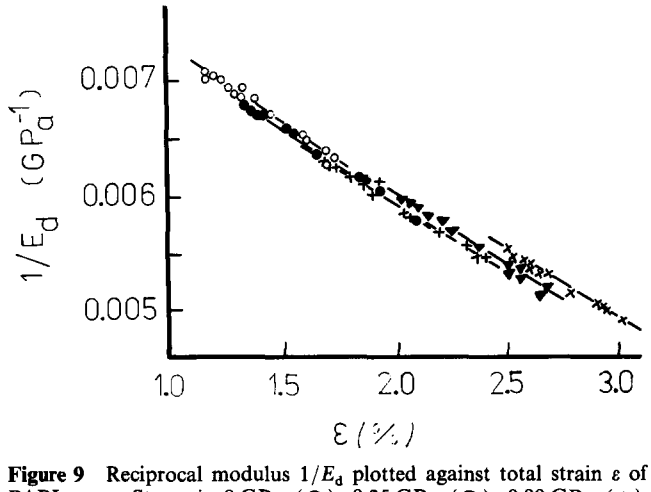

Figure 9 Reciprocal modulus $1/E_d$ plotted against total strain ε of PABI yarn. Stress is 0 GPa (○), 0.25 GPa (●), 0.90 GPa (+), 1.35 GPa (▼) and 2.24 GPa (×)

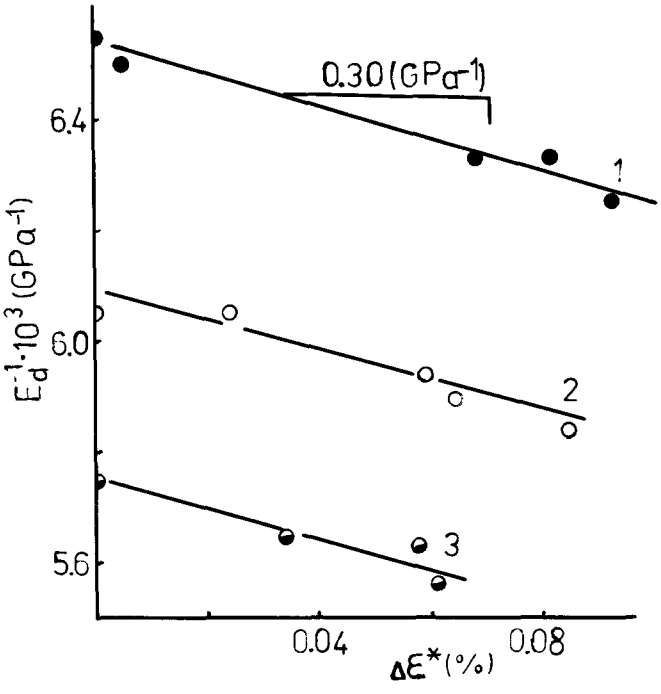

Figure 10 Reciprocal modulus $1/E_d$ of PPTA yarn plotted against increment of strain during creep: $T = 110°C$; stress is 0.38 (1), 0.63 (2) and 0.88 GPa (3)

connected in series, and each fragment may be in one of two energy states with different rigidities (*Figure 12*); (2) the molecular stress is invariable along its length; (3) interaction between molecules is very weak.

Let us denote the stiffness of the fragments in these states as E_1 and E_2 respectively (the stiffness of fragments may be described by 'soft' and 'stiff' springs). It is natural to suppose that the 'stiff' state corresponds to straightened molecules in high-modulus crystalline regions and the 'soft' state is a defect of crystallite structures, which in oriented polymers is supposed to be a molecular kink[20,21] (*Figure 12*). The transition of some fragments from the low-modulus ('defect') state to the high-modulus state under load leads to an increase in the chain length and increase in the rigidity. Recovery is the reverse transition, leading to a decrease in modulus. Creep in this model leads to some increase in the degree of crystallization of the polymer under stress.

Creep and recovery may also be described as a reversible chemical reaction of the first order. If n_1 and n_2 are parts of soft and stiff fragments, then:

$$n_1 + n_2 = 1 \tag{3}$$

The Young's modulus of springs connected in series (*Figure 12*) is given by:

$$1/E = n_1/E_1 + n_2/E_2 \tag{4}$$

If dn_2 fragments pass from defect ('soft') to main ('rigid') state, the chain elongation is:

$$d\varepsilon^* = x_0\, dn_2/D \tag{5}$$

where x_0 is the elongation of one fragment during this transition (*Figure 12*) and D is the fragment length. Taking into account equations (3)–(5), an increase in modulus due to this transition may be written:

$$\frac{1}{E} = \frac{1}{E_0} - \frac{(E_2 - E_1)D}{E_1E_2x_0}\Delta\varepsilon^* \tag{6}$$

Equations (6) and (1) coincide if:

$$K = (E_2 - E_1)D/E_1E_2x_0$$

Hence, this model explains the linear dependence of the reverse Young's modulus on creep elongation.

CREEP RATE

The rate of the chain transition from the defect energy state to the main one is given by:

$$dn_1/dt = -k_1n_1 + k_2n_2 \tag{7}$$

where k_1 and k_2 are rate constants for creep and for recovery transitions, which may be defined from the Eyring equation[22]:

$$k_1 = \omega_0 \exp[(-U^+ + v_0\sigma)/RT]$$

$$k_2 = \omega_0 \exp[(-U^- - v_0\sigma)/RT]$$

U^+ and U^- are activation energies for creep and

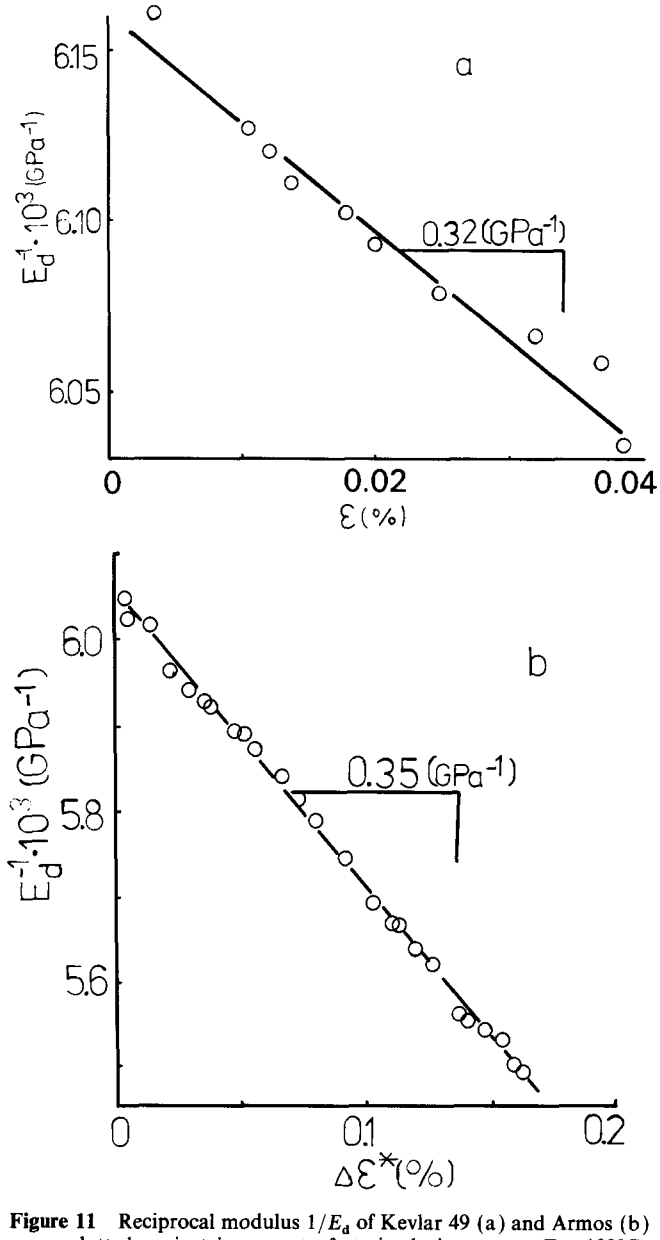

Figure 11 Reciprocal modulus $1/E_d$ of Kevlar 49 (a) and Armos (b) yarns plotted against increment of strain during creep: $T = 100°C$; creep stress is equal to 1.25 GPa for Kevlar 49 and 1.42 GPa for Armos fibres respectively

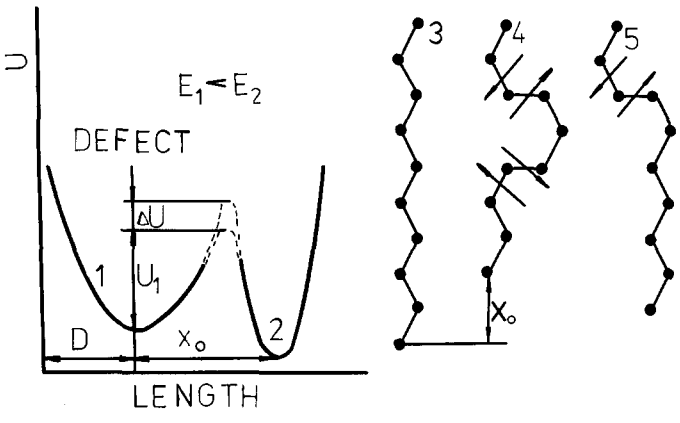

Figure 12 The model. Potential energy of polymer fragment: x_0 is the chain elongation during transition from the first to the second state, D is the mean fragment length, U_1 is the lower level of the activation energy of transition, ΔU is the width of the activation energy zone. On the right are shown: (3) a schematic representation of the straightened polymer chain (main energy state); (4) a pair of kinks; (5) a single kink equivalent to a shear defect of the chain; arrows show shear direction

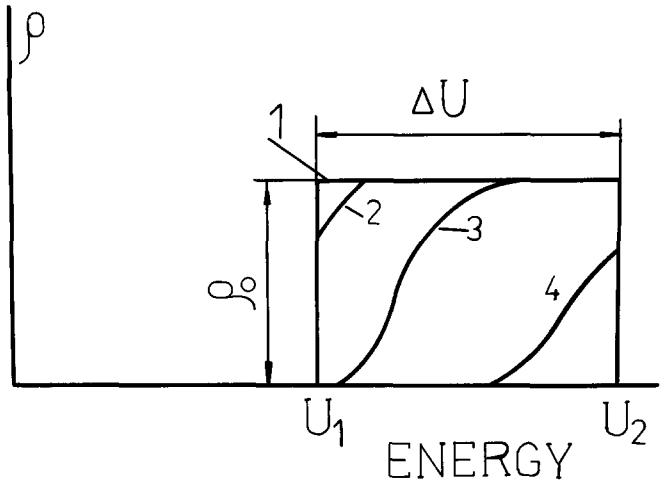

Figure 13 Distribution of activation energies for the transition at different time ranges: (1) rectangular distribution at initial moment $t = 0$; (2, 3, 4) 'short', 'intermediate' and 'long' periods of creep time. U_1 and U_2 are lower and upper levels of the zone

recovery; ω_0 is the fragment vibration frequency; v_0 is the activation volume; σ is the tensile stress; and R is the gas constant. The solution of equation (7) is:

$$n_1 = \frac{k_2}{k_1 - k_2} + \left(n_1^0 - \frac{k_2}{k_1 - k_2}\right) \exp[-(k_1 - k_2)t] \quad (8)$$

where n_1^0 is the part of 'defect' fragments at $t = 0$.

This solution predicts the exponential decrease of creep rate with time. In fact, an exponential law of creep with time is not observed and usually $\Delta\varepsilon^* \sim \ln t$. At first sight, a logarithmic creep law contradicts the model of two energy states.

It should be noted that, for any transition in solid-state bodies, a distribution in activation energies and the existence of energy zones are typical. So let us suppose that the activation energy of the transition is not constant for all fragments, and some distribution of activation energies exists. For simplicity, a rectangular distribution of activation energies in the zone (*Figure 13*) will be considered. If the height and the length of the zone are ρ_0 (density of distribution) and ΔU, then $n_1^0 = \rho_0 \Delta U$. Supposing that the rate of the creep transition is much higher compared with the reverse transition ($k_1 \gg k_2$), equation (8) may be rewritten in the following way:

$$\rho(U, t) = \rho_0 \exp[-t\omega_0^{-1} \exp(-U/RT)]$$

Consequently:

$$d\rho(U, t)/dt = -\rho_0 \omega_0 \exp(-U/RT) \times \exp[-t\omega_0^{-1} \exp(-U/RT)]$$

Integrating:

$$\frac{dn_1}{dt} = \int_{U_1}^{U_2} \frac{d\rho(U, t)}{dt} dU$$

we have:

$$\frac{dn_1}{dt} = -\frac{RT\rho_0}{t}\left\{\exp\left[-k_0 t \exp\left(-\frac{\Delta U}{RT}\right)\right] - \exp(-k_0 t)\right\} \quad (9)$$

where $k_0 = \omega_0^{-1} \exp(-U_1/RT)$, U_1 and U_2 are the bottom and the upper levels of the zone, $\Delta U = U_1 - U_2$.

Analysis of equation (9) shows that creep laws are essentially different in three time ranges. (1) At short periods of time ($t \ll t_1 = 1/k_0$) the transition rate is:

$$dn_1/dt = -\rho_0 k_0 RT[1 - \exp(-\Delta U/RT)]$$

Hence the creep rate is constant. (2) If $t_1 \ll t \ll t_2$ (where $t_2 = t_1 \exp(\Delta U/RT)$), then the transition rate is:

$$dn_1/dt = -\rho_0 RT/t$$

and elongation $\Delta\varepsilon^*$ is proportional to log of time. It is worth mentioning that the creep rate in this time range does not depend on stress and is directly proportional to temperature. (3) If $t \gg t_2$ then the rate of creep decreases exponentially. Thus the creep rate is constant in the first time range, decreases as $1/t$ in the second and decreases exponentially in the third. Note that in 'short' and 'long' time ranges the creep rate is exponentially dependent on stress and temperature. On the contrary, in the intermediate time range when $\Delta\varepsilon^* \sim \ln t$, the dependence of creep rate on stress and temperature is not described by Boltzmann's exponent.

Additional analysis shows that the log dependence of creep elongation on time in the second time range is quite insensitive to the zone shape in the initial moment (i.e. to ρ distribution for $t = 0$). For example, $\Delta\varepsilon^*$ is proportional to $t \ln t$ even if, for $t = 0$, $\rho \sim (U - U_1)^2$. Thus because the supposition that the activation energy is described by the zone is very natural for solid-state bodies, the log creep law does not contradict the model.

DISCUSSION

A kink is considered to be a molecular shear defect, analogous to a dislocation in crystalline materials (part 5, *Figure 12*). The straightening of a kink requires a shift of a significant part of the molecule with respect to the rest of the polymer. However, this supposition is doubtful. Subsequently we suppose that the defect state is a pair of molecular kinks as shown in *Figure 12* (part 4). In this case the transition from the defect to the main state is the annihilation of a pair of kinks, which does not require the movement of a significant part of the molecule. This transition may be the result of the movement of kinks along the chain as well as the rotation

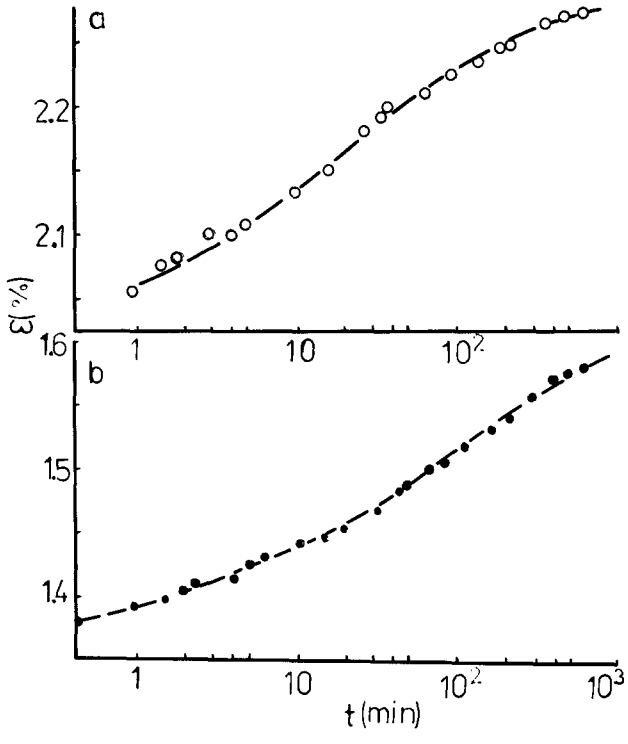

Figure 14 PABI (a) and Armos (b) fibre elongation during creep plotted against log time. PABI: $\sigma = 100$ GPa, $T = 110$°C. Armos: $T = 100$°C, $\sigma = 1.42$ GPa

of some molecular group around two chemical bonds (part 4, *Figure 12*).

The effect of concentration of dislocations (kinks in polymers) on the Young's modulus of crystals and oriented polymers is different. In crystals, variation of dislocation concentration leads to a comparatively low change of elasticity. The opposite is true in oriented polymers, where molecular defects essentially affect the Young's modulus.

According to *Figure 14* at high stresses and elevated temperature the dependence of $\Delta\varepsilon^*$ on $\ln t$ for PABI (a) and Armos (b) fibres declines from a straight line and can be described by S-like curves. In spite of this the $1/E_d$ *versus* $\Delta\varepsilon^*$ correlation remains linear (*Figure 11b*). Thus we can conclude that creep is associated with the same transition at 'short' and 'long' times despite different relaxation times. The insignificant dependence of K on stress and temperature also confirms this supposition.

The possibility to consider only two energy states may be explained by the high degree of polymer orientation and the high part of straightened fragments. Because of this the polymer may be considered as a crystal with defects. Another consequence of high orientation is the respectively low difference between the fibre Young's modulus (130–215 GPa) and its theoretical limit (210–250 GPa[15,16]). Of course, to describe creep of less oriented polymers with chains in the form of balls, more than two energy states may be needed.

In this model the molecular stress is considered constant along its length. The foundation for this is the high anisotropy of fibre properties. The degree of anisotropy could be described by the ratio of the stress in the chain to intermolecular interaction, γ. For aramid fibres shear and longitudinal strengths are equal to 40–45 MPa[23] and ~4.0 GPa respectively. Hence the ratio of longitudinal to transverse strengths is equal to ~100 and γ is estimated as 100. As a result of the high anisotropy, the molecule end is not loaded in some zone[24,25], the length of which (so-called ineffective length) is denoted as L_c. In this zone the molecule is gradually loaded from zero stress at the end to undisturbed stress, σ_f, far from the end. In the shear lag approximation[25], L_c may be roughly evaluated as $L_c \sim a\gamma \simeq 100a$, where a is the typical length of a chemical bond in a polymer chain (C–C or C–N). Since the length of a C–C or C–N bond is equal to approximately 2 Å, $L_c \simeq 200$ Å. Thus, the molecule may be loaded only at a length $L > 200$ Å. Analogously, far from the molecule end, stress could not be reduced significantly unless the length of the defect is not higher than L_c. The shorter defects, for example kinks, are not able to change the molecular stress significantly.

If the material is perfectly elastic and its modulus is constant, then strain and stress are not independent. The relation between stress and strain is described by Hooke's law. Analogously, if in a viscoelastic body the Young's modulus and the creep strain are related by equation (1), then stress, strain and the Young's modulus are not independent. Hence, the Young's modulus could be determined from the stress and strain during deformation if the constant K is known.

The total strain in a non-elastic body is equal to the sum of elastic, viscoelastic (including the 'fast' transitions with low activation energies) and irreversible components. Since the irreversible part of the deformation in our experiments was negligible, the total increase of the modulus under loading is a result of elastic and viscoelastic components:

$$d\varepsilon = d\varepsilon_e + d\varepsilon^* \tag{10}$$

where $d\varepsilon_e$ and $d\varepsilon^*$ are the differentials of elastic and viscoelastic components of total strain.

Hooke's law gives:

$$d\sigma = E\, d\varepsilon_e \tag{11}$$

An increase of modulus due to viscoelastic strain may be described by:

$$d\varepsilon^* = d(\sigma/E) \tag{12}$$

Now we can consider deformation of PABI fibres in *Figure 1*. The initial stress, strain and modulus in *Figure 1* are equivalent to $\varepsilon_0 = 0.8\%$, $\sigma_0 = 0$, $E_0 = 130$ GPa. Parameter K is equal to 0.12 GPa^{-1}. If the final stress and strain are $\sigma_f = 2.15$ GPa and $\varepsilon_f = 3.0\%$ respectively, then by solving the system of equations (1) and (10)–(12) numerically, we obtain a final value for the modulus as approximately 160 GPa. This value differs significantly from the experimental value of 215 GPa. If an increase in the Young's modulus were due solely to inelastic deformation, total fibre elongation would be significantly higher than $\varepsilon_f - \varepsilon_0 = 2.2\%$. Hence we conclude that the observed increase in PABI fibre modulus could not be explained solely by the effect of viscoelastic strain, and there should be some other causes leading to an increase in the modulus. The second cause of the increase of the modulus is the effect of the elastic part of the deformation due to the non-parabolic shape of the energy curve (*Figure 12*) and the bending of fibrils[10]. The effect cannot result solely from the elastic or from the viscoelastic strains, but its nature is the combined effect of viscoelastic and elastic strains. Equations (11)–(13) allow for estimation of the parts of these effects. The viscoelastic

part of the total strain leads to about 30% of the total increase in PABI fibre modulus (from 130 to 215 GPa), and 70% of the effect is a result of elastic strain. An analogous consideration shows that in PPTA and Kevlar 49 fibres the creep results in about 30% and in Armos about 45% of the total modulus growth.

CONCLUSIONS

Drying of fibre leads to its elongation and to some increase in the Young's modulus. The same is true for the effect of fibre irreversible strain.

Creep leads to an increase of Young's modulus of PABI, Kevlar 49, Terlon and Armos fibres up to 215, 195, 190 and 205 GPa respectively (80–95% of the theoretical limit).

Some of the difference between moduli values obtained by the acoustic and mechanical methods is due to fibre creep. If the creep rate is slow, the difference between these values may be neglected.

The dependence of the reciprocal Young's modulus on the creep strain may be described as a straight line. The slope of this straight line does not depend on the creep stress and temperature.

Fibre creep and recovery may be described as a thermoactivated transition between two energy states. In these states the polymer chain may be described by a 'soft' and a 'stiff' spring respectively. The 'soft' and 'rigid' states are supposed to be the straightened molecule and a pair of molecular kinks, and the latter are analogous to a pair of dislocations in crystalline materials.

If the activation energy of the transition between these states has some distribution, i.e. it is described by an energy zone, the creep strain dependence on time is logarithmic.

ACKNOWLEDGEMENTS

The authors are grateful to Drs L. J. Vladimirov, S. N. Chvalun and E. S. Zelenskii and to Professors A. A. Berlin, L. I. Manevich and A. S. Argon for stimulating discussions.

REFERENCES

1 Bessonov, M. I. and Rudakov, A. P. *Vysokomol. Soed.* (*B*) 1971, **13**, 542
2 Abramchuk, S. S. *Mechanica Komp. Materialov* 1986, 387
3 Slutsker, L. I., Ismonkulov, K., Chereiskii, Yu. Z., Dobrovolskaja, I. P. and Mirzoev, O. *Vysokomol. Soed.* (*A*) 1988, **30**, 424
4 Rogozinsky, A. K. and Turusov, R. A. in 'Fracture and Strength of Heterogeneous Materials' (Ed. A. M. Leksovski), Physical Technical Institute, USSR Academy of Sciences, Leningrad, 1985, p. 80 (in Russian)
5 Abramchuk, S. S., Dimitrienko, I. P. and Kisilev, V. N. in 'Diagnosis Methods of Bearing Capacity of Composites', Zinatne, Riga, 1983, p. 102 (in Russian)
6 Rogozinsky, A. K., Bazhenov, S. L. and Zelensky, E. S. *Vysokomol. Soed.* (*B*) 1990, **32**, 437
7 Ericksen, R. H. *Polymer* 1985, **26**, 733
8 Northolt, M. G. *Polymer* 1980, **21**, 1199
9 Northolt, M. G. and v. d. Hout, R. *Polymer* 1985, **26**, 310
10 Allen, S. R. and Roche, E. J. *Polymer* 1989, **30**, 996
11 Ballou, J. W. *Polym. Prep.* 1976, **17**, 75
12 Penn, L. and Milanovich, F. *Polymer* 1979, **20**, 31
13 v. d. Zvaag, S., Northolt, M. G., Young, R. J., Robinson, I. M., Galiotis, C. and Batchelder, D. N. *Polymer* 1987, **28**, 276
14 Budnitskii, G. A. *J. Mendeleev Chem. Soc.* 1989, **34**, 438
15 Slutsker, L. I., Utevskii, L. E., Chereiskii, Yu. Z. and Perepelkin, K. E. *J. Polym. Sci., Polym. Symp. Edn.* 1977, **58**, 339
16 Gaymans, R. G., Tijssen, J., Harkama, S. and Bantjes, S. *Polymer* 1976, **17**, 517
17 Takayanagi, M. *Proc. 4th Int. Congr. Rheology, Part 1* (Eds. E. H. Lee and A. L. Copley), Wiley, New York, 1975, p. 161
18 Chvalun, S. N., Zubov, Yu. A. and Bakeev, N. F. *Vysokomol. Soed.* (*B*) 1989, **31**, 834
19 Peterlin, A. in 'Ultra-High Modulus Polymers' (Eds. A. Ciferri and I. M. Ward), Applied Science, London, 1981, Ch. 10, p. 181
20 Robertson, R. E. *J. Chem. Phys.* 1966, **44**, 3950
21 Blasenbrey, S. and Pechhold, W. *Rheol. Acta* 1967, **6**, 176
22 Eyring, H. *J. Chem. Phys.* 1936, **4**, 283
23 Bazhenov, S. L., Kozey, V. V., Berlin, A. A., Kuperman, A. M., Zelenskii, E. S. and Lebedeva, O. V. *Dokl. Akad. Nauk* 1988, **303**, 1155
24 Capaccio, G., Gibson, A. G. and Ward, I. M. in 'Ultra-High Modulus Polymers' (Eds. A. Ciferri and I. M. Ward), Applied Science, London, 1981, Ch. 1, p. 5
25 Rosen, B. W. and Dow, N. F. in 'Fracture', Vol. 7 (Ed. H. Liebovitz), Academic Press, New York, 1972, p. 300